Improved Energy Coupling of Human P-glycoprotein by the Glycine 185 to Valine Mutation[†]

Hiroshi Omote, Robert A. Figler, Mark K. Polar, and Marwan K. Al-Shawi*

Department of Molecular Physiology and Biological Physics, University of Virginia Health System, P.O. Box 800736, Charlottesville, Virginia 22908-0736

Received August 1, 2003; Revised Manuscript Received January 28, 2004

ABSTRACT: A glycine 185 to valine mutation of human P-glycoprotein (ABCB1, MDR1) has been previously isolated from high colchicine resistance cell lines. We have employed purified and reconstituted P-glycoproteins expressed in *Saccharomyces cerevisiae* [Figler et al. (2000) *Arch. Biochem. Biophys. 376*, 34−46] and devised a set of thermodynamic analyses to reveal the mechanism of improved resistance. Purified G185V enzyme shows altered basal ATPase activity but a strong stimulation of colchicine- and etoposide-dependent activities, suggesting a tight regulation of ATPase activity by these drugs. The mutant enzyme has a higher apparent K_m for colchicine and a lower K_m for etoposide than that of wild type. Kinetic constants for other transported drugs were not significantly modified by this mutation. Systematic thermodynamic analyses indicate that the G185V enzyme has modified thermodynamic properties of colchicine- and etoposide-dependent activities. To improve the rate of colchicine or etoposide transport, the G185V enzyme has lowered the Arrhenius activation energy of the transport rate-limiting step. The high transition state energies of wild-type P-glycoprotein, when transporting etoposide or colchicine, increase the probability of nonproductive degradation of the transition state without transport. G185V P-glycoprotein transports etoposide or colchicine in an energetically more efficient way with decreased enthalpic and entropic components of the activation energy. Our new data fully reconcile the apparently conflicting results of previous studies. EPR analysis of the spin-labeled G185C enzyme in a cysteine-less background and kinetic parameters of the G185C enzyme indicate that position 185 is surrounded by other residues and is volume sensitive. These results and atomic detail structural modeling suggest that residue 185 is a pivotal point in transmitting conformational changes between the catalytic sites and the colchicine drug binding domain. Replacement of this residue with a bulky valine alters this communication and results in more efficient transport of etoposide or colchicine.

Multidrug resistance (MDR) is a one of the greatest challenges to current medical sciences. Tumor cells exhibiting cross-resistance to multiple anticancer drugs are often associated with higher expression of the 170 kDa P-glycoprotein, *MDR1* gene product (*1*). Several lines of evidence indicate that this protein is responsible for drug resistance through extrusion of drugs from the interior of cells.

Human P-glycoprotein (Pgp)[1] is a member of the ATP binding cassette (ABC) transporter superfamily (*2*). ABC proteins are one of the largest protein families and are involved in transporting a wide variety of biological compounds across the membrane (*3*). P-glycoprotein is a plasma membrane protein which consists of two homologous halves; each half contains transmembrane and nucleotide binding domains. P-glycoprotein transports various and structurally unrelated compounds to the outside of cells driven by the energy of ATP hydrolysis (*4*). ATPase activity of this enzyme is stimulated severalfold by transported drugs. Most of the transport substrates are hydrophobic, and many have positive charge. Because of hydrophobicity, drugs partition into lipid bilayers or bind tightly to proteins and chromosomes and have low free concentrations in the cytosol. In the "hydrophobic vacuum cleaner model", P-glycoprotein takes its substrates from the inner leaflet of the plasma membrane and transports them out to the extracellular bulk water phase (*1*). Unique features of P-glycoprotein are its broad substrate specificity and basal ATPase activity in the absence of transport substrates. Despite the great medical importance of this protein, the actual mechanism of drug transport is still not well understood. Recently, we established a new thermodynamic approach to reveal the transport energetics of this protein (*5*). We found that basal and drug-related

[†] Supported by NIH Grant GM52502 to M.K.S.

* Corresponding author. Tel: (434) 243-8674. Fax: (434) 982-1616. E-mail: ma9a@virginia.edu.

[1] Abbreviations: Cys(−), cysteine-less P-glycoprotein; DFP, diisopropyl fluorophosphate; DDM, *n*-dodecyl β-D-maltopyranoside; *E. coli* lipid, ether/acetone-precipitated *Escherichia coli* lipid; EDTA, ethylenediaminetetraacetic acid; EGTA, ethylene glycol bis(β-aminoethyl ether)-*N*,*N*,*N*′,*N*′-tetraacetic acid; G185V, glycine 185 to valine substitution; k_{cat}, turnover number; K_m^{ATP}, apparent Michaelis constant for ATP activation; K_m^D, apparent Michaelis constant for drug activation; K_i, drug inhibition constant; LFER, linear free energy relationship; PC, phosphatidylcholine; Pgp, P-glycoprotein; PMSF, phenylmethanesulfonyl fluoride; PS, phosphatidylserine; SL-verapamil, spin-labeled verapamil; V_b, apparent V_{max} for basal ATPase activity; V_d, apparent V_{max} for drug-dependent ATPase activity.

10.1021/bi035365l CCC: $27.50
Published on Web 03/11/2004

ATPase activities have different thermodynamic characteristics and concluded that basal activity is an uncoupled cycle while drug-related ATPase activity is a drug-transport-coupled cycle. Regulation of activity between these two cycles makes P-glycoprotein an energy-inefficient transporter sacrificing efficiency to achieve higher drug clearance rates (*5*).

Chemical selections of cancer cell lines generally yield higher resistance to the selecting drug as well as pleiotropic cross-resistance to other drugs, frequently due to amplification of P-glycoprotein expression (*1*). Choi et al. (*6*) reported that KB carcinoma cell lines which were selected for colchicine became more resistant to colchicine but not to vinblastine. It was later found that the amount of P-glycoprotein expressed on the plasma membranes of these cells was the same as in the parental KB cells. Increased specificity and resistance to colchicine indicated an altered transport mechanism of P-glycoprotein in these selected cells (*7*). Interestingly, the selected cell lines had a P-glycoprotein mutated at position 185 (glycine 185 to valine, G185V), and this mutation is now believed to be responsible for high colchicine resistance. Stein et al. (*8*) did demonstrate that cells expressing G185V P-glycoprotein had a decreased rate of colchicine uptake when compared to cells with wild-type P-glycoprotein. Although details of the improved resistance afforded by G185V P-glycoprotein are still not clear, it is highly correlated with the colchicine transport mechanism. Therefore, this mutant is of great interest for understanding the mechanism of drug transport by P-glycoprotein. In this report, we applied thermodynamic analyses to this mutant enzyme, employing purified and reconstituted systems. Our results indicate a unique energy-coupling mechanism of P-glycoprotein.

MATERIALS AND METHODS

Plasmids. To construct a human P-glycoprotein expression plasmid which carries the glycine 185 to valine mutation, part of pSK1.MDR (*9*) was transferred to a wild-type expression plasmid YEpMDR1HIS (*10*). A 4100 bp fragment of *Sac*II/*Xho*I digests of pSK1.MDR which has a valine codon at position 185 was cloned to pBluescriptIISK to generate RAF19. pBSEcoRIMDR was constructed by cloning a 2110 bp *Eco*RI fragment of YEpMDR1HIS to pBluescriptIISK+, and a 744 bp *Nco*I/*Nsi*I fragment of the resultant plasmid was replaced by the corresponding fragment of RAF19. This plasmid was named pBSMDREcRIfragV185. YEpV185MDR10xHis was constructed by replacing the *Eco*RI fragment of YEpMDR1HIS with the corresponding fragment of pBSMDREcRIfragV185. This plasmid has the DNA sequence corresponding to region His61−Ala308 of pSK1.MDR.

YEpMDR1HISΔCys which encodes a histidine-tagged cysteine-less enzyme was created by transferring a *Nco*I/*Bsm*I segment of cysteine-less P-glycoprotein gene into YEpMDR1HIS. A plasmid containing a cysteine-less P-glycoprotein [Cys(−) Pgp] gene in which the seven native cysteines were replaced by alanines was kindly provided by Dr. D. M. Clarke (*11*). To construct YEpMDR1HISΔCys, a 1205 bp *Eco*RI/*Bam*HI fragment of YEpMDR1His was cloned into pBluescriptKS+, and a *Nco*I/*Nsi*I fragment of the resultant plasmid was replaced by a corresponding region of the cysteine-less gene (pBScys(−)). Also, a *Xho*I/*Nsi*I fragment from YEpMDR1His was inserted into the resultant pBluescriptKS+ plasmid followed by a *Nco*I/*Bsm*I segment replacement by the same region of the cysteine-less gene to generate a plasmid which has a *Nco*I/*Bsm*I fragment of cysteine-less gene and a *Bam*HI/*Nco*I fragment of YEpMDR1HIS. Finally, YEpMDR1HISΔCys was created by replacing the *Bam*HI/*Bsm*I fragment of YEpMDR1His with the corresponding fragment of the intermediate plasmid. Complete sequencing of this Cys(−) Pgp revealed that it contained the naturally occurring single nucleotide polymorphism G2677T [alanine 893 to serine (*12*)].

YEpMDR1HisΔCysG185C (glycine 185 to cysteine) and YEpMDR1HisΔCysR588C (arginine 588 to cysteine) were generated by PCR mutagenesis using a set of primers (AAGATTAATGAATGTATTGGTGACAAA and TTTGTCACCAATACATTCTTATAATTC, forward and reverse, respectively, for G185C, GTGATAGCTCATTGTTTGTCTACAGTT and AACTGTAGACAAACAATGAGCTATCAC for R588C).

Yeast Strain and Media. Protease-deficient *Saccharomyces cerevisiae* strain BJ5457 was grown under synthetic dextrose medium (*13*) for expressing P-glycoproteins in the presence of 10% (v/v) glycerol as a chemical chaperone as described previously (*10*).

Purification of P-glycoprotein. Wild-type and mutant P-glycoproteins were expressed in yeast plasma membranes. The initial step of purification entailed a fractionation of a plasma membrane enriched microsomal fraction ("highly enriched plasma membranes") by the method of Perlin et al. (*14*). Yeast-expressed P-glycoproteins were fully active and had high specific activities similar to those obtained when these proteins were expressed in their native mammalian cells (*10*). Purification and reconstitution of P-glycoprotein from plasma membranes into liposomes were carried out as described previously (*10*) with the following adaptations. In this study, three types of reconstitution lipids were employed. For type 1 lipids [previously called "mixed lipids" (*10*)], the Ni-NTA column pH 8 washing step was done with 0.1% mixed lipid stock composed of 61% *Escherichia coli* ether/acetone-precipitated lipid (Avanti, no. 100600), 17% frozen egg yolk PC (Sigma no. P7318), 10% bovine brain PS (Folch fraction III; Sigma, no. B1627) and 12% cholesterol (Sigma, no. C8667). Elution of P-glycoprotein off the Ni-NTA column was performed at pH 7.4 in the presence of 0.4% "mixed lipid" stock. For type 2 lipids, the column-washing step was performed with 0.1% *E. coli* lipid stock. Column elution was done with 0.4% lipid stock composed of 58% *E. coli* lipid, 19% fresh egg yolk PC (Sigma, no. P3556), 10% bovine brain PS, and 13% cholesterol. For type 3 lipids the pH 8 column-washing step was performed with 0.2% lipid stock composed of 60% *E. coli* lipid, 17.5% frozen egg yolk PC, 10% bovine brain PS, and 12.5% cholesterol *E. coli* lipid stock. Column elution was done with 0.1% of the column-washing lipid stock above. In all cases proteoliposomes were made by dialysis as previously described (*15*).

Cysteine mutant P-glycoproteins used for spin-labeling studies were purified by a slightly modified procedure as follows. After Pgp was adsorbed by a Ni-NTA resin (Qiagen), the column was washed by 10 volumes of a buffer

comprised of 25 mM Tris−SO_4, pH 8.0, 20% (v/v) glycerol, 50 mM Na_2SO_4, 2 mM NaATP, 1 mM $MgSO_4$, 1 mM β-mercaptoethanol, 5 mM imidazole, 1 mM PMSF, 2 μM pepstatin A, 1 μM leupeptin, and 1 mM benzamidine. The buffer additionally contained 1.4% *n*-octyl β-D-glucopyranoside and 0.1% type 1 lipids (see above). A second wash with 10 volumes of the same buffer but now containing 2 mM *n*-dodecyl β-D-maltopyranoside followed. P-glycoprotein was eluted with 4 volumes of elution buffer comprised of 25 mM Tris−SO_4, pH 7.5, 20% glycerol, 50 mM Na_2SO_4, 2 mM NaATP, 1 mM $MgSO_4$, 1 mM β-mercaptoethanol, 250 mM imidazole, 1 mM PMSF, and 2 mM DDM. After addition of fresh 2 mM DTT, solublized Pgp was concentrated by an Amicon stirred cell with an XM50 membrane to ~1.0 mg/mL and stored at −80 °C until use.

Spin Labeling of Enzyme. Purified solubilized cysteine mutant enzymes were passed through a PD-10 gel filtration column (Amersham-Pharmacia) at 4 °C equilibrated with a buffer containing 50 mM Tris-HCl, pH 7.5, 20% glycerol, 140 mM NaCl, 5 mM $MgCl_2$, and 2 mM DDM. After addition of 5 mM ADP, 200 μM proxylmaleimide (Aldrich) was added to the mixture, and the resultant mixture was incubated for 3 h at 25 °C. The reaction mixture was passed through another PD-10 column equilibrated with a buffer containing 50 mM MES−NaOH, pH 6.5, 20% glycerol, 140 mM NaCl, 5 mM $MgCl_2$, and 0.3 mM DDM to remove excess unreacted probe and detergent. After addition of 5 mM ADP, type 1 lipids (see above) prepared with DDM were added at a lipid-to-protein ratio of 25 by weight. The mixture was diluted 5-fold with dilution buffer containing 50 mM MES−NaOH, pH 6.5, 20% glycerol, 140 mM NaCl, and 5 mM $MgCl_2$. Then it was dialyzed for 10 h against 1 L of dialysis buffer comprised of 50 mM Tris-HCl, pH 7.5, 5 mM $MgCl_2$, 140 mM NaCl, and 0.5 g/L Bio-Beads SM-2. The buffer was renewed and the dialysis continued for a further 10 h. Proteoliposomes were harvested by centrifugation at 184000*g* for 3 h and resuspended in a small amount of dialysis buffer.

EPR Measurements. EPR spectra were measured at 23 °C using a Bruker EMX X-band EPR spectrometer equipped with a loop gap resonator. Protein samples were concentrated to about 40 μM in the EPR buffer (50 mM Tris-HCl, pH 7.5 at 23 °C, 5 mM $MgCl_2$, 140 mM NaCl) before measurements and loaded into TPX capillaries (IGC Medical Advances Inc.).

Assays. Standard ATPase assays were performed in 40 mM Tris−SO_4 (pH 7.4), 10 mM NaATP, 15 mM $MgSO_4$, 0.1 mM EGTA, 2 mM NaN_3, and 1% DMSO (v/v) at 37 °C in the presence and absence of transport drugs as indicated in the text. Samples (50 μL) were removed at appropriate times (four time points to ensure linearity) and injected into 1 mL of ice- cold 8 mM EDTA (pH 8) to stop the reaction. Liberated P_i was determined by the method of Van Veldhoven and Mannaerts (*16*) as modified by Al-Shawi et al. (*17*).

Kinetic and Thermodynamic Analyses. Drug titration curves were fitted with an activity-partitioning model as described earlier (*18*). In this model, P-glycoprotein partitions its activity between an uncoupled basal activity cycle or a coupled activity cycle depending on drug concentration (see Figure 6). The steady-state ATPase activity was fitted by the following equation to obtain the kinetic constants (*5*):

$$v = \{V_b + ((V_d - V_b)[\text{drug}]/(K_m^D + [\text{drug}]))\}\{1 - ([\text{drug}]/(K_i + [\text{drug}]))\} \quad (1)$$

Here, v is the ATPase activity, [drug] is the drug concentration, V_b is the maximal basal ATPase activity (apparent V_{max}) in the absence of drug, V_d is the maximal ATPase activity (apparent V_{max}) in the presence of drug, K_m^D is the Michaelis constant for drug activation, and K_i is the inhibition constant for drug inhibition. The kinetic constants K_m^D, K_i, V_b, and V_d were obtained by fitting drug titration data with this equation.

Intrinsic thermodynamic parameters at pH 7.5 for drug transport at saturating ligand concentrations were obtained from Arrhenius assays for drug and ATP titrations as detailed elsewhere (*5*). Briefly, assays were performed in Arrhenius cocktails comprised of 50 mM Na-HEPES (pH 7.5), 10 mM NaATP, 17 mM $MgSO_4$, 1% DMSO (v/v), 5 mM K-phosphoenolpyruvate, and 32 μg/mL pyruvate kinase. ATPase assays were performed as above at 2 deg increments from 23 to 35 °C. Each ATPase cocktail was adjusted to pH 7.5 at each temperature by using a pH meter that was accurately calibrated at each temperature. Apparent activation energies and entropic and enthalpic components at a given temperature were calculated from the slopes and intercepts of plots of ln k_{cat} versus $1/T$ as previously described (*19*). These apparent thermodynamic parameters were converted to absolute thermodynamic parameters as previously described (*5*) by utilizing apparent K_m^{ATP} values and apparent K_m^D values. Apparent K_m^D values were determined at each temperature for each Pgp preparation type in the Arrhenius cocktails as described above. Apparent K_m^{ATP} values were determined at each temperature for each Pgp preparation type and drug used. The Arrhenius cocktails above were mixed with varying amounts of 50 mM Na-HEPES (pH 7.5), 7.1 mM $MgSO_4$, 1% DMSO (v/v), 5 mM K-phosphenolpyruvate, and 32 μg/mL pyruvate kinase to achieve the following ATP concentrations (at nearly constant free Mg^{2+}): 0, 0.1, 0.2, 0.5, 0.8, 1, 2, 5, 8, and 10 mM Mg·ATP. The data of the ATPase assays were fit to the Michaelis−Menten equation to obtain the apparent K_m^{ATP} values. Examples of the variation of K_m^{ATP} with temperature are shown in Figure 1.

RESULTS

Drug Dependence of G185V ATPase Activity. Human G185V mutant P-glycoprotein was overexpressed in yeast plasma membranes using our yeast expression system in the presence of 10% glycerol as a chemical chaperone (*10*). Plasma membrane levels and yields of the purified and reconstituted protein were the same as the wild-type protein, indicating no obvious folding problems (results not shown). We have found that misfolded P-glycoproteins are rapidly ubiquitinated and subsequently degraded, leading to substantially lowered yields (*10*).

We have recently established, by rigorous experimental analyses, that P-glycoprotein has two different types of ATPase activity, an uncoupled basal ATPase and a coupled drug-related activity (*5*). These activities are independent but are interrelated by the fraction of P-glycoprotein partitioning to either the uncoupled basal cycle or the drug-dependent

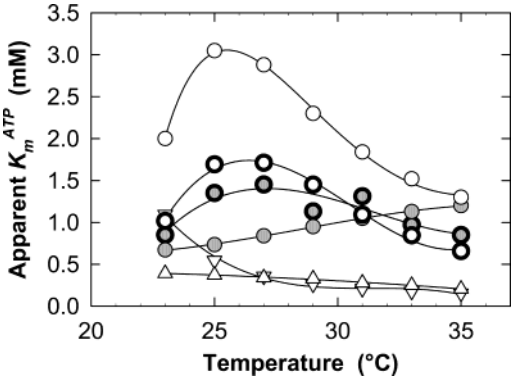

FIGURE 1: Variation of apparent K_m^{ATP} as a function of temperature. P-glycoprotein ATPase activities in the presence and absence of transport drugs were determined as a function of Mg·ATP concentration and temperature. Assays were performed at pH 7.5 in the presence of an ATP regeneration system (see Materials and Methods for details). Examples of calculated K_m^{ATP} values for P-glycoprotein in type 1 lipids for different transport substrates are plotted as a function of temperature. Plotted lines are arbitrary. Symbols: shaded ○, WT basal (no drug present); △, WT and 130 μM valinomycin; ▽, WT and 130 μM verapamil; ○, WT and 2 mM colchicine; shaded thick ○, G185V basal; thick ○, G185V and 5 mM colchicine. WT data are from ref *5*.

coupled transport cycle. In the absence of transport drugs, all activity occurs through the uncoupled cycle. However, in the presence of saturating transport drug concentrations all of the activity follows the coupled drug-transport cycle with no underlying basal activity. Very recently, Rao and Nuti demonstrated that these two P-glycoprotein states have two distinct conformations (*20*). Ramachandra et al. (*21*) previously reported altered kinetics of plasma membrane ATPase activity of cells expressing the G185V mutant Pgp, including a higher basal ATPase activity. We tested the colchicine dependence of ATPase activity using purified P-glycoproteins reconstituted into transport-competent proteoliposomes (*18*) employing type 1 lipids (see Materials and Methods). There were marked differences between wild-type and G185V enzymes. Basal activity of G185V Pgp was reduced to 28% of basal wild-type activity (Figure 2 legend) although both enzyme activities were strongly stimulated by colchicine. G185V Pgp appeared to be more tightly regulated than wild type (Figure 2A). Surprisingly, the apparent affinity for colchicine was decreased by the mutation (contrast with ref *22*). On the other hand, the apparent affinity for etoposide was increased (Figure 2B, Table 1) as previously observed (*23*). Kinetic constants, summarized in Table 1, were obtained by fitting such drug titration curves using the partitioning model of ATPase activity described above.

Apparent kinetic constants are highly condition-dependent and can only be compared when exactly the same conditions are employed (*5*). This fact can be easily ascertained in Figure 1, where the apparent K_m^{ATP} values vary significantly as a function of temperature. Apparent affinities to other drugs were not drastically altered by the mutation (Table 1). Under the conditions of Table 1, the K_m^D for colchicine was increased 8.5-fold by mutation without a significant change of K_i. The apparent K_m^D for etoposide was decreased 4.4-fold by the G185V mutation. The apparent specificity constant, k_{cat}/K_m^D, at saturating colchicine was reduced slightly from 4.0×10^3 to 1.1×10^3 M^{-1} s^{-1} by the G185V mutation. These results indicate that improved resistance to colchicine is not due to increased drug affinity. In contrast, the apparent specificity constant for etoposide was increased from 2.2×10^3 to 1.7×10^5 M^{-1} s^{-1} by the G185V mutation. Although the apparent specificity constants change in opposite directions by the G185V mutation for colchicine and etoposide, it will be shown later that the same underlying mechanism of improved drug transport applies to both drugs. The apparent value of K_m^D is a rough estimate of the dissociation constant (K_d) for the drug and represents a virtual dissociation constant of the drug from all enzyme species (*18, 5*). For instance, when WT P-glycoprotein was reconstituted in purified asolectin, K_m^D values of 1.9 μM and 0.73 mM were obtained for valinomycin and colchicine, respectively. K_d values of 0.35 μM and 1.1 mM were obtained for valinomycin and colchicine, respectively, when similar preparations were assayed for direct drug binding by the fluorescence method of Liu and Sharom (*24*) employing 2-(4-maleimidoanilino)naphthalene-6-sulfonic acid (MIANS) reacted P-glycoprotein.

We employed our new thermodynamic approach (*5*) to analyze the mechanism of improved resistance. It is noteworthy that the apparent ratio of V_d of colchicine-dependent coupled ATPase to V_b (basal ATPase activity) in type 1 lipids was increased from 2.8 to 15 by the valine substitution, suggesting a more strict regulation of ATPase activity. Krupka (*25*) has postulated, and we have verified (*5*), that this ratio (when calculated at infinite substrate concentrations as in Table 2) can be used as a crude indication of the relative strength of interaction of drug binding to the coupling transition state (ternary complex). On this basis, it appears that G185V Pgp binds colchicine tightly in the coupling transition state. However, it must be emphasized here that the ratio of V_d/V_b is not an absolute indicator of the strength of interaction of drug binding to the coupling transition state. This arises from the fact that basal ATPase activity and drug-dependent coupled activity are on two separate reaction cycles with two independent transition states (*5*) that can be modulated independently. In a sense, the commonly used term "drug-stimulated ATPase activity" is a misnomer in that P-glycoprotein activity partitions between two independent cycles. A more relevant term would be "drug-transport-related ATPase activity" (see ref *5* for further verification of this statement). As will be shown later, modulation of the absolute value of the V_d/V_b ratio is possible by changing the reconstitution conditions without affecting the underlying conclusions discussed in this paper.

Thermodynamic Properties. For any single type of chemical reaction, there is a linear free energy relationship between the log of turnover rates at two different temperatures. This relationship can be used to distinguish between transition states of different reactions. Thus log plots of activities at different temperatures can show if reactions have similar transition state structures (*5*, *26*). The intrinsic velocities for the various preparations were calculated for saturating ATP and saturating activating drug (if present) as detailed in Materials and Methods, having corrected for the inhibitory effect of excess drugs (*5*). In Figure 3, coupled ATPase activities (open symbols) and uncoupled basal ATPase activities (shaded symbols) were located on different lines [$p < 0.001$ (*5*)]. This indicates that the two activities have different rate-limiting transition states. When G185V Pgp etoposide- or colchicine-dependent ATPase activities were plotted on Figure 3, they were located on the line for drug-

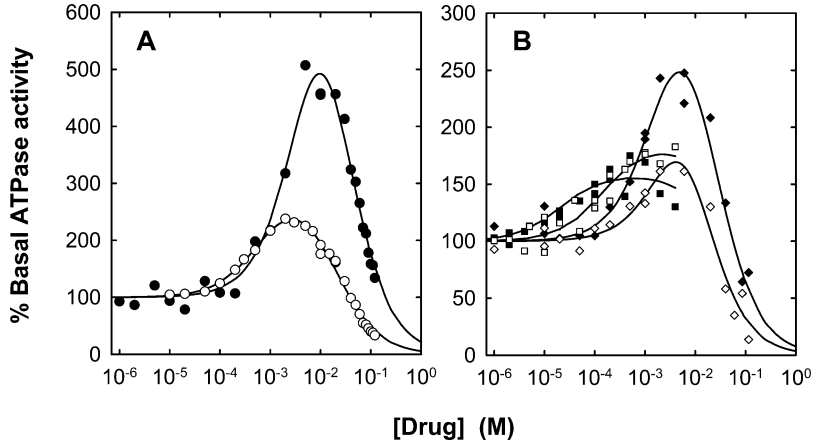

FIGURE 2: Drug activation and inhibition of P-glycoprotein ATPase activity. Drug-dependent ATPase activities were measured at pH 7.4 and 37 °C as described in Materials and Methods and plotted as a function of log drug concentration. Representative examples are plotted for P-glycoprotein preparations reconstituted in type 1 lipids. Curves drawn are least squares regression fits of the data to eq 1. Kinetic constants derived from such plots are reported in Table 1. 100% basal ATPase activity values (V_b) were 0.90, 0.25, 0.55, and 0.18 μmol (mg of P-glycoprotein)$^{-1}$ min^{-1} for WT, G185V, Cys(−), and G185C/Cys(−) P-glycoproteins, respectively. Panel A: ○, WT plus colchicine; ●, G185V plus colchicine. Panel B: □, WT plus etoposide; ■, G185V plus etoposide; ◇, Cys(−) plus colchicine; ◆, G185C/Cys(−) plus colchicine.

Table 1: Apparent Kinetic Constants of ATPase Activity of WT, Cysteine-less, and G185 Mutant P-glycoproteins[a]

	verapamil				valinomycin[b]			colchicine				etoposide[b]		
enzyme	K_m^D (μM)	V_d (U/mg)[d]	V_d/V_b[c] (fold)	K_i (mM)	K_m^D (μM)	V_d (U/mg)	V_d/V_b (fold)	K_m^D (μM)	V_d (U/mg)	V_d/V_b (fold)	K_i (mM)	K_m^D (μM)	V_d (U/mg)	V_d/V_b (fold)
WT	62	5.7	6.4	0.64	2.0	3.7	4.1	680	2.5	2.8	18	145	1.3	1.4
G185V	64	1.6	6.4	1.0	3.3	1.1	4.2	5800	3.6	15	20	33	1.7	6.8
Cys(−)[e]	2.1	0.96	1.6	0.87	0.60	1.3	2.3	410	1.4	2.8	30			
G185C/Cys(−)	5.3	0.46	2.6	1.5	1.2	0.30	1.7	1900	0.71	3.9	18			

[a] Conditions were as follows: Standard ATPase activities were measured at 37 °C, pH 7.4, and 10 mM Mg·ATP. Kinetic constants were obtained by fitting drug titration curves to eq 1. All P-glycoprotein preparations assayed in this table were reconstituted in type 1 lipids. [b] The K_i values for valinomycin or etoposide could not be determined due to their limited aqueous solubility. These drugs precipitated at lower concentrations than those required for binding to the low-affinity drug binding sites. [c] V_d/V_b represents the fold change of the apparent ATPase activation calculated from the fits of eq 1. These values are highly condition dependent and are only useful for comparisons of results assayed employing exactly the same conditions. [d] Activity units of U/mg correspond to μmol (mg of Pgp)$^{-1}$ min^{-1}. [e] Cys(−) represents cysteine-less P-glycoprotein where all seven cysteines were changed to alanines (*11*).

transport-related ATPase activities. This means that etoposide- and colchicine-dependent ATPase activities of the G185V mutant enzyme have a rate-limiting transition state similar to that of other drug-transport-related coupled activities. They became very similar to the valinomycin and verapamil drug-transport-related activities observed with WT Pgp (Figure 3). Since the transition state structures were similar, there were no gross conformational perturbations by this mutation. In contrast, the etoposide- and colchicine-dependent ATPase activities of WT Pgp were located at the intersection of coupled and uncoupled activity lines.

Enthalpic ($\Delta H^{\ddagger}$) and entropic ($T\Delta S^{\ddagger}$) components of activation energies were calculated by Eyring's rate theory as previously described (*19*). The *intrinsic* thermodynamic parameters of the rate-limiting transition state were calculated for saturating ATP and saturating activating drug as detailed in Materials and Methods (*5*), having been corrected for the inhibitory effect of excess drugs. The calculated data are shown in Table 2. Results are most easily visualized as an isokinetic plot (Figure 4). The rate-limiting transition state plotted was shown to be related to a conformational change associated with the reorientation of drug binding sites from high-affinity on sites to low-affinity unloading sites (see Figure 6 and ref *5*). Points in the upper right corner have large enthalpic and large compensating entropic components of activity, indicating that enzymes in this area of the graph need a large number of bond rearrangements (formed and broken) to reach the coupling transition state. On the other hand, points at the opposite corner of Figure 4 require less bond rearrangements to establish the coupling transition state. Although wild-type activities with valinomycin and verapamil (both good transport substrates of human P-glycoprotein) were located in the center of this figure, the etoposide- and colchicine-dependent activities were in the upper right corner. Apparently, wild-type etoposide- or colchicine-dependent activities each need a large number of bond rearrangements to achieve the coupling transition state. This indicates that etoposide or colchicine are poor substrates for this enzyme. However, the G185V mutation shifted the etoposide- and colchicine-dependent activities toward the lower left corner (Figure 4). This shows that the G185V mutant enzyme requires fewer bond rearrangements than the wild type to reach the coupling transition state when transporting these two drugs. The G185V mutation turns etoposide and colchicine into excellent transport substrates for this enzyme form.

Contributions of the *intrinsic* enthalpic and entropic components for the coupling transition state of etoposide- or colchicine-dependent activities are shown in Table 2. For etoposide transport in type 1 lipids, enthalpy was reduced

Table 2: Intrinsic Drug-Transport Rates and Corrected Transition State Thermodynamic Parameters for Steady-State Activity of WT, Cysteine-less, and G185 Mutant P-glycoproteins[a]

enzyme	lipid type[b]	transport drug	transport rate[c] (s^{-1})	basal rate (V_b) (s^{-1})	stimulation[d] (V_d/V_b) (fold)	$\Delta H^{\ddagger}$ (kJ mol^{-1})	$T\Delta S^{\ddagger}$ (kJ mol^{-1})	$\Delta G^{\ddagger}$ (kJ mol^{-1})
WT	type 1	none (basal)		1.9		104.8	30.9	73.9
WT	type 1	colchicine	2.2		1.2	121.8	48.3	73.5
WT	type 1	etoposide	2.1		1.1	159.5	85.8	73.7
G185V	type 1	none (basal)		0.77		67.2	−9.0	76.2
G185V	type 1	colchicine	6.6		8.6	105.4 (−16.4)[e]	34.7 (−13.6)	70.7 (−2.8)
G185V	type 1	etoposide	4.3		5.6	93.1 (−66.4)	21.3 (−64.5)	71.8 (−1.9)
Cys(−)	type 1	none (basal)		1.6		127.3	53.0	74.3
Cys(−)	type 1	colchicine	3.6		2.2	145.6	73.3	72.2
G185C/Cys(−)	type 1	none (basal)		2.0		68.0	−5.7	73.3
G185C/Cys(−)	type 1	colchicine	5.2		2.6	98.6 (−47.0)	27.3 (−46.0)	71.3 (−0.9)
WT	type 2	none (basal)		3.7		134.9	62.7	72.2
WT	type 2	colchicine	4.3		1.2	136.2	64.4	71.8
G185V	type 2	none (basal)		2.9		107.9	35.1	72.8
G185V	type 2	colchicine	8.5		2.9	111.9 (−24.3)	41.8 (−22.6)	70.1 (−1.7)
WT	type 3	none (basal)		2.6		102.4	29.3	73.1
WT	type 3	colchicine	5.6		2.1	121.5	50.4	71.1
G185V	type 3	none (basal)		5.5		97.6	26.5	71.1
G185V	type 3	colchicine	12.2		2.2	104.5 (−17.0)	35.4 (−15.0)	69.1 (−2.0)

[a] Intrinsic values were calculated at 35 °C, pH 7.5, with saturating Mg·ATP and saturating transport drug if present. [b] See Materials and Methods for types of lipids and reconstitution conditions employed. [c] Transport rate is the intrinsic turnover number for the coupled activity cycle. [d] Intrinsic V_{max} values for saturating substrates (V_d, V_{max} for drug-dependent ATPase activity; V_b, V_{max} for basal ATPase activity). [e] Values in parentheses are differences between parameters for the mutant enzymes (185V or 185C) and their corresponding G185 parental type.

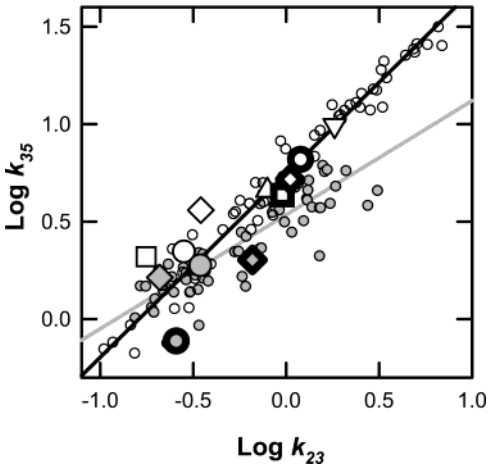

FIGURE 3: Linear free energy relationships of basal and drug-transport-related ATPase activities. ATPase activities of P-glycoprotein preparations with and without drugs were measured at 23 and 35 °C at pH 7.5 in the Arrhenius ATPase cocktails described in Materials and Methods. Basal ATPase activities in the absence of transport drugs are illustrated by gray shaded symbols. Drug-dependent ATPase activities are illustrated by open symbols. The small symbols show data taken from ref *5* for human wild-type P-glycoprotein (MDR1) and Chinese hamster P-glycoprotein (PGP1) reconstituted with type 1 lipids or *E. coli* lipids in the presence or absence of seven different P-glycoprotein transport substrates. The large symbols show the intrinsic ATPase activities at saturating ATP and drug if present for the P-glycoprotein types used in this study reconstituted in type 1 lipids. Large symbols: shaded ○, WT basal; ○, WT plus colchicine; □, WT plus etoposide; △, WT plus valinomycin; ▽, WT plus verapamil; shaded thick ○, G185V basal activity; thick ○, G185V plus colchicine; thick □, G185V plus etoposide; shaded ◇, Cys(−) basal; ◇, Cys(−) plus colchicine; shaded ◇ (thick line), G185C/Cys(−) basal; ◇ (thick line), G185C/Cys(−) plus colchicine. Gray and black lines were fitted to the points with and without drugs, respectively. The two lines are statistically significantly different ($p < 0.001$).

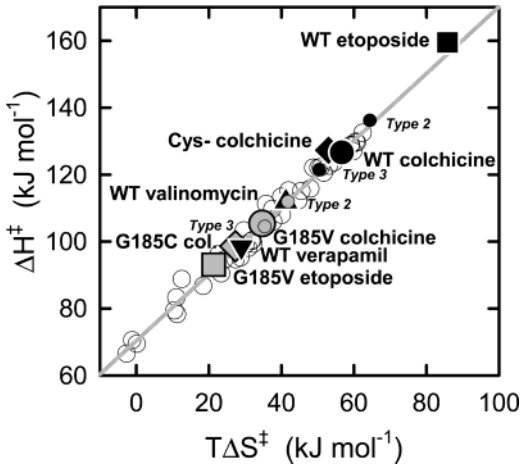

FIGURE 4: Isokinetic plot of drug-transport-related activity. Intrinsic $\Delta H^{\ddagger}$ and $T\Delta S^{\ddagger}$ values of drug-transport-related activities at pH 7.5 and 35 °C for saturating ligand concentrations (saturating ATP and saturating activating drugs) were calculated as described in Materials and Methods. Activities were calculated for saturating concentrations of drugs without the inhibitory effect of excess drugs (*5*). The open symbols show data taken from ref *5* for human wild-type P-glycoprotein (MDR1) and Chinese hamster P-glycoprotein (PGP1) reconstituted with type 1 lipids or *E. coli* lipids for various transport substrates. The large filled symbols are for P-glycoproteins reconstituted in type 1 lipids. Small filled symbols have the type of lipid used indicated on the plot. Black symbols show P-glycoproteins containing glycine at position 185. Gray symbols show mutant forms of P-glycoprotein at position 185. Symbols: ●, WT with colchicine; ■, WT with etoposide; ▲, WT with valinomycin; ▼, WT with verapamil; shaded ○, G185V with colchicine; shaded □, G185V with etoposide; ◆, Cys(−) with colchicine; shaded ◇, G185C/Cys(−) with colchicine.

by the mutation by 66.4 kJ mol^{-1} to achieve the coupling transition state. Entropy was also decreased 64.5 kJ mol^{-1} by the mutation. Similarly, for colchcine transport, enthalpy was reduced by the mutation by 16.4 kJ mol^{-1} to achieve the coupling transition state. Entropy was also decreased 13.6 kJ mol^{-1} by the mutation. Thus, the majority of decreased enthalpy is compensated by decreased entropy and results in a small difference of Gibb's free energy ($\Delta G^{\ddagger}$) of the coupling transition state. The *intrinsic* Gibb's free energy

of etoposide-dependent activity is decreased from 73.7 to 71.8 kJ mol^{-1} by mutation. Similarly, $\Delta G^{\ddagger}$ of colchicine-dependent activity is decreased from 73.5 to 70.7 kJ mol^{-1} by mutation. The lowered values of $\Delta H^{\ddagger}$ and $T\Delta S^{\ddagger}$ on mutation indicate that the number of bond alterations is decreased and less conformational change is needed to achieve the coupling transition state. These results confirm that the major effect of the G185V mutation is in the improved catalytic efficiency for etoposide or colchicine transport.

Effects of Modulating the Basal ATPase Activity. We have previously shown that the type of lipid employed in reconstitution has profound effects on the basal ATPase activities of different types of P-glycoprotein (*5*). To ensure that our results and interpretations were valid, we reconstituted wild-type and G185V P-glycoproteins in three types of lipid preparations (see Materials and Methods for details). The basal activities for wild-type P-glycoprotein, when assayed using the conditions of Table 1, were 0.9, 1.4, and 1.0 μmol (mg of P-glycoprotein)$^{-1}$ min^{-1} for type 1, 2, and 3 lipids, respectively (1.5-fold range), whereas the basal activities for G185V P-glycoprotein were 0.25, 1.2, and 2.2 μmol (mg of P-glycoprotein)$^{-1}$ min^{-1} for type 1, 2, and 3 lipids, respectively (9-fold range). Thus, it appears that the G185V mutation is more sensitive than WT Pgp to the type of lipid in the membrane and in lipid control of the flux through the uncoupled basal cycle. Nevertheless, when the intrinsic thermodynamic parameters were calculated for colchicine-dependent activity of G185V and compared to WT Pgp, there was always improved colchicine transport by the mutation in any lipid type (Table 2). Thus, enthalpy was always decreased, compensated by decreased entropy and a net reduction of $\Delta G^{\ddagger}$, by the mutation in all lipid types employed. This fact is easily visualized in Figure 4.

Drug Transport by Wild-Type and Mutant P-glycoproteins. For highly membrane-permeable drugs such as colchicine, it is theoretically not feasible to obtain valid kinetics of drug transport by P-glycoprotein in proteoliposomes by direct assay (see Discussion in ref *27* and ref *25*). To overcome such obstacles, we previously devised a spin-labeled verapamil analogue (SL-verapamil) that had an extremely low flip-flop rate in membranes, thus allowing valid kinetic data to be obtained (*18*). Unfortunately, as verapamil transport is not affected by the mutations employed in this study (Table 1), spin-labeled verapamil could not be used to see the effects of the mutations on transport. Thus, drug transport needed to be assessed by a different method. To do this, we calculated the intrinsic values of the maximal flux rates for the coupled activity cycle for the different P-glycoprotein forms with the different drug substrates employed (Table 2). Such flux rates give a good representation of the maximal rate of drug transport achievable by a given enzyme form (see also ref. *25*). We have previously validated this assertion by employing WT Pgp and comparing the flux rates obtained by the strict transport assay employing SL-verapamil in the EPR spectrometer with those calculated by the partitioning of ATPase activity between basal and transport-dependent activity (*5*, *18*). In Table 2 it can be seen that the transport rates of etoposide and colchicine were increased by 2- and 3-fold, respectively, in type 1 lipids for G185V Pgp compared to WT Pgp. Similarly, a 2-fold increase in the rate of colchicine transport by G185V Pgp in type 2 and type 3 lipids was observed (Table 2).

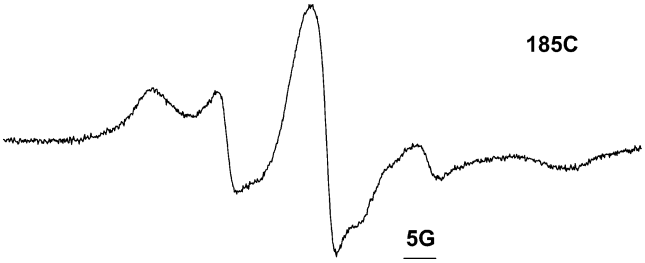

FIGURE 5: EPR spectra of spin-labeled G185C. G185C/Cys(−) P-glycoprotein was spin-labeled with proxylmaleimide as described in Materials and Methods, and the EPR spectrum was measured.

Mobility of Spin Probe Attached to Cysteine 185. In many cases, a highly conserved glycine is found in a critical region of a protein peptide chain that needs flexibility. Most P-glycoproteins have glycine or alanine at position 185, suggesting the importance of this residue for protein conformation. Replacement of this residue with bulky side chains may restrict such flexibility and result in altered kinetics. We tested this idea by introducing a cysteine residue at position 185 and by measuring the mobility of a spin probe attached to it. The G185C mutant enzyme was made on the Cys(−) background in which all seven cysteines were changed to alanines (*11*). Colchicine-dependent activities of G185C/Cys(−) and Cys(−) enzymes are shown in Figure 2B and are qualitatively similar to the pattern seen with G185V when compared to wild-type P-glycoprotein (Figure 2A). Kinetic constants of G185C/Cys(−) and Cys(−) enzymes are summarized in Table 1. ATPase activities of the Cys(−) enzyme were lower than those for the wild type as was previously observed (*28*, *29*). Interestingly, the apparent affinities to drugs were increased. After this study was completed, we sequenced the entire Cys(−) cDNA of Loo and Clarke (*11*). We found that it contained the naturally occurring single nucleotide polymorphism G2677T (alanine 893 to serine) present in 62% of European Americans which has been associated with enhanced drug clearance of fexofenadine (*12*). Nonetheless, replacing glycine 185 with cysteine in this Cys(−) background (containing a total of eight other point substitutions) still increased K_m^D for colchicine and also increased the extent of ATPase activation (Table 1). Overall, the situation was quite similar to the G185V mutation compared against wild-type Pgp (Table 1). Furthermore, G185C/Cys(−) when compared to the parental Cys(−) enzyme behaved in a fashion similar to G185V compared to wild-type Pgp on the LFER plot (Figure 3). Additionally, for colchicine-transport-dependent ATPase activity, the replacement of the glycine by a cysteine led to an enthalpy reduction of 47.0 kJ mol^{-1} compensated by an entropy reduction of 46.0 kJ mol^{-1} and a net $\Delta\Delta G^{\ddagger}$ value of −0.9 kJ mol^{-1} (Table 2). Thus, G185C/Cys(−) Pgp transports colchicine more efficiently than Cys(−) Pgp, as can be discerned in Figure 4. In addition, the rate of colchicine transport increased by 1.4-fold (Table 2).

The width of the center peak of a nitroxide EPR signal is highly sensitive to the mobility of the probe, and it is correlated with the location of the probe within the protein (*30*). Figure 5 shows a representative EPR spectrum of spin-labeled G185C/Cys(−). Importantly, this modified enzyme retained up to 84% of the ATPase activity of the unmodified form. The center peak width of spin-labeled G185C/Cys(−) enzyme was approximately 4.2 ± 0.14 G (±standard error).

This is too large a value for a freely rotating probe. This result indicates that the spin probe attached to Cys185 is surrounded by other residues and its mobility is sterically restricted. For comparison, the partially buried spin-labeled R588C/Cys(−), which is located near the surface region of the catalytic domain (see Figure 7), showed a smaller center peak width (3.7 ± 0.04 G). In the case of the G185C-SL enzyme there was no significant change in spin-label motional freedom on the addition of ATP, drug, or ATP plus drug, further demonstrating the restricted position of the G185C residue. In contrast, for R588C-SL, the mobility of the spin probe increased in the presence of ATP ($\Delta\Delta H_0 = -0.11$ G) and stayed nearly constant with drugs ($\Delta\Delta H_0 = +0.01$ G for verapamil) but was the most mobile in the presence of both ligands ($\Delta\Delta H_0 = -0.28$ G).

DISCUSSION

A majority of enzymes encountered in biology have high substrate specificity and good catalytic efficiency (*31*). In this regard, P-glycoprotein is a unique enzyme that appears to lack these typical features. The unusual properties of this protein may correlate with its special function as a multidrug transporter. However, implications of these unusual features on the mechanism of drug transport are not clear yet. In this context, a combination of mutagenic and thermodynamic approaches would be a good protocol to probe the unique mechanism of P-glycoprotein.

The P-glycoprotein G185V mutant was first isolated from highly colchicine-resistant cell lines (*6*). Cell lines having G185V Pgp exhibit higher resistance to colchicine and etopside but a decreased resistance to vinblastine, Taxol, and actinomycin D, suggesting altered drug specificity (*7*, *32*, *33*). The high resistance to colchicine was thought to have originated from altered kinetics of the mutant enzyme since there was increased colchicine extrusion from cells without a concomitant change in plasma membrane G185V Pgp expression levels (*7*, *21*, *33*). Thus, G185V Pgp is of great interest for understanding the mechanism of drug specificity and transport. Rao reported that the mutant enzyme had increased activation of ATPase activity by colchicine and increased affinity to colchicine (*22*). He concluded that these features were directly correlated with higher resistance. On the other hand, Roninson and co-workers reported reduced affinity of G185V to colchicine based on a P-glycoprotein conformation-specific antibody (*33*). This was consistent with the result of decreased labeling by a photoaffinity colchicine analogue (*7*). On the basis of these results, they illustrated the mechanism in which residue 185 is close to the drug-releasing site, and replacement of this residue with valine facilitates the colchicine release, resulting in improved transport. Although there are many extensive studies with natural membrane preparations, unified conclusions cannot be made due to apparently conflicting data. It was difficult to analyze the real kinetics of mutant P-glycoprotein due to the use of complex whole cell systems or impure natural membrane preparations. Our recent development of a P-glycoprotein overexpression system together with a purification and reconstitution system makes it possible to investigate detailed mechanisms (*10*). In contrast to previous works, here we used purified preparations for systematic kinetic and thermodynamic analyses.

Our work established several points. First, G185V Pgp has a lowered apparent affinity to colchicine and decreased basal ATPase activity in type 1 lipids (Figure 2A, Table 1). In contrast, the apparent affinity for etoposide in type 1 lipids was increased by the mutation (Figure 2B, Table 1). Maximal ATPase activity attained at optimal colchicine concentration was lower than that of wild type (calculated from Figure 2A data). This clearly indicates that apparent affinity or velocity changes do not explain the improved colchicine transport. The change of K_m^D reflects the change of drug binding sites (see Results; see also refs *18* and *5*) rather than a change of releasing sites as was postulated by Safa et al. (*7*). Thus, an alternate mechanism must be operating.

Second, the activation energies of the coupling transition state were reduced by the G185V mutation for etoposide or colchicine transport (Table 2). More importantly, both the enthalpic and entropic components of the transition state were decreased (Table 2, Figure 4). This implies a need for fewer bond rearrangements to establish the coupling transition state in the mutant enzyme. The G185V enzyme appeared to bind etoposide or colchicine tighter in the transition state than wild type (see Results). Taken together, these results show that G185V Pgp increased etoposide or colchicine transport through an energetically more efficient transport mechanism. This enzyme establishes such high efficiency by several ways. P-glycoprotein has two different catalytic cycles (*5*): one is the coupled drug transport cycle and another is the uncoupled basal activity (Figure 6, basal activity). A different uncoupling mechanism was previously described by Krupka (*25*). Reduced basal activity (Figure 2 legend) and a large colchicine activation fold of turnover by G185V Pgp (Table 1) indicate that G185V Pgp ATPase activity is tightly regulated. G185V P-glycoprotein has lowered activation energy of the coupling transition state and binds etoposide and colchicine tighter in this state than the wild type (Figure 4). Together, these effects decrease the possibility of a nonproductive decay of the transition state by an energy-dissipating pathway (failed transport; Figure 6). Lowered entropic and enthalpic components of the activation energy suggest that G185V Pgp establishes the coupling transition state with less bond reorganization. Such small bond rearrangements reduce the necessary energy interconversions (conformational changes required), thus decreasing the probability of energy dissipation on crossing the transition state. The G185V mutation transits the transition state for etoposide and colchicine transport faster than the wild type (Table 2) as would have been expected from the discussion above. A decreased concentration of the transition state further protects the enzyme from unexpected degradation of high-energy structures without transport (failed transport; Figure 6). The net result is a more efficient transport of colchicine by G185V Pgp. A similar situation to G185V compared to wild-type Pgp was previously seen when the wild-type enzyme was compared to the γ-M23K mutant of *E. coli* ATP synthase (*34*, *35*). Thermodynamic analysis of the γ-M23K mutant enzyme indicated that an increased activation energy of the γ-subunit rotation (rate-limiting coupling step) created a new energy-dissipating pathway and resulted in an uncoupled phenotype.

Our conclusions are also supported by the fact that expression of G185V Pgp increases extrusion of colchicine from cells (*7*, *8*, *21*). Since, expression levels of P-

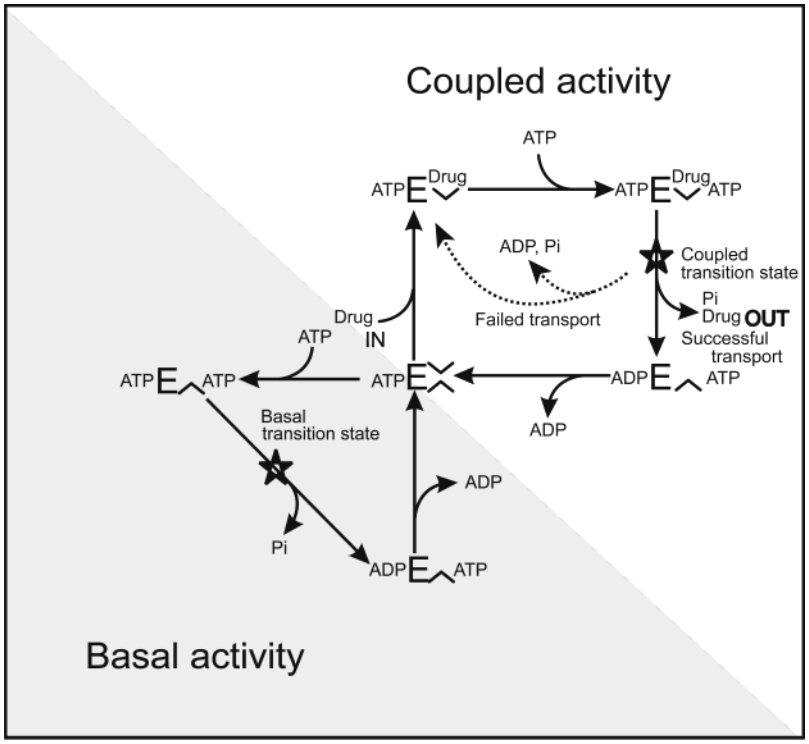

FIGURE 6: Catalytic cycles of P-glycoprotein. A partitioning model of P-glycoprotein catalytic cycles is shown (see ref *5* for a rigorous experimental proof of this model). Upper right cycle, drug-transport-related coupled activity; lower left cycle, uncoupled basal activity. If two ATP molecules bind in the absence of bound drug, then P-glycoprotein partitions to the uncoupled cycle and hydrolyzes ATP without any transport work. However, if there is a sufficient amount of transport drug present, P-glycoprotein partitions to the coupled activity cycle. The coupled cycle is an alternating catalytic cycle previously described (*4*). Transport drug binds first followed by ATP to form the ternary complex. After being passed through the high-energy transition state, drug is released to the other side of the membrane (successful transport). Different transport drugs lead to different energy levels of the rate-limiting coupling transition state (*5*). Due to the instability of the higher energy transition states, there is a greater probability of nonproductive transition state decay without drug transport (failed transport).

glycoprotein were not affected by the G185V mutation, the net colchicine transport rate must have been increased by the G185V mutation. Such increased transport rates were seen here (Table 2). However, such an effect of G185V Pgp was specific for etoposide or colchicine and was not observed for verapamil or valinomycin in our experiments (Table 1). As shown in Figure 4, different drugs have different *intrinsic* activation energies and related thermodynamic components which reflect a different efficiency of transport for each drug (*5*). In addition, there is no apparent correlation between K_m^D and V_{max} of these drugs (Table 1). These facts suggest that P-glycoprotein does not use drug binding energy to facilitate transport. Most likely, P-glycoprotein obtained broad drug specificity at the expense of a loss of drug binding energy utilization to drive transport. The G185V mutation specifically makes etoposide and colchicine into substrates that are more efficient for transport. Interestingly, a similar case has been reported for lactose permease (*36*). In contrast to G185V mutation, the A177V mutation of lactose permease leads to broad substrate specificity at the cost of an uncoupled phenotype.

The apparent discrepancies, among results seen when other kinetic studies are compared to each other (see introduction and above) and to this highly controlled study, have trivial explanations that can now be easily reconciled. We have previously shown (*5*) that the kinetics of P-glycoprotein can be described by a modified "general modifier mechanism" of Botts and Morales (*37*) as illustrated in Figure 6. As discussed in Al-Shawi et al. (*5*), fitting the data to other models will lead to different values of apparent kinetic constants. When one ligand (ATP or drug) is set to a fixed concentration and the other ligand is varied, as is the usual practice, apparent Michaelis−Menten kinetics obtain. However, in the modified general modifier mechanism (Figure 6) a transport drug acts as a hyperbolic activator or inhibitor of total P-glycoprotein ATPase activity. ATP itself acts as a hyperbolic activator of drug transport or transport-dependent ATPase activity (*5*). An immediate consequence of this is that apparent kinetic constants will vary widely between different experiments if the conditions of assay are not absolutely the same. An example of this can be seen in Figure 1 where the apparent K_m^{ATP} values for different P-glycoproteins and drug types vary significantly as a function of temperature. Natural polymorphisms with different drug specificities are also quite common in human P-glycoproteins isolated from different sources (*12*) as was discovered for the Cys(−) enzyme employed in this study (see Materials and Methods and Results). Finally, and most importantly for this study, the type of lipid membrane in which P-glycoprotein finds itself modulates the partitioning between the basal and coupled activity cycles as well as modulating the absolute activity values (see Results and Table 2). Furthermore, the extent of this partitioning varies with different P-glycoprotein types (see Results, Table 2, and ref *5*). Additionally, G185V Pgp basal activity is particularly sensitive to the lipid makeup of the membrane and could be modulated by up to 9-fold in our experiments (see Results and Table 2). Such a large variation encompasses the range

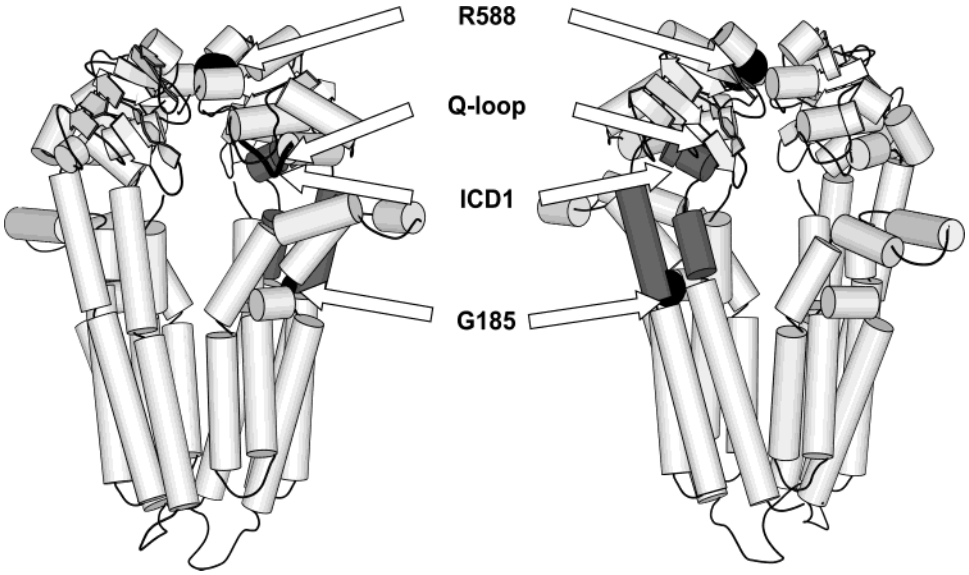

FIGURE 7: Structural model of P-glycoprotein based on the MsbA crystal structure. Front and back views of homology-modeled human P-glycoprotein. The *V. cholera* lipid A half-transporter MsbA is homologous with each half of Pgp (~27% identity). We have used the 3.8 Å crystal structure of MsbA (*43*; PDB 1PF4) and the 1.5 Å crystal structure of HisP (*44*; PDB 1B0U) to model the structure of Pgp. Homology modeling was carried out using MODELLER (*56*). The first step was to align Pgp halves with MsbA and HisP by CLUSTALX (*57*). Initially, sequences of *V. cholera* MsbA (residues 10−564) and human Pgp N-terminal residues (34−637) and C-terminal residues (694−1279) were aligned. Transmembrane domain alignment was verified by secondary structure analysis by PHD (*58*) and PROF (*59*) and was manually adjusted on the basis of the location of gaps and Gly, Pro, Trp, and Tyr residues. A missing part of the MsbA crystal structure (residues 203−237) was modeled as a helix−loop−helix as predicted by PHD. P-glycoprotein nucleotide binding domains (residues 391−637 and 1034−1280) were modeled using the coordinates of HisP. During modeling, atom conflicts were removed by simulated annealing from 1000 to 300 K. Modeled nucleotide binding domains and transmembrane domains were assembled and fit into the corresponding regions of MsbA. Locations of residues Gly185 and Arg588 are indicated by filled balls. Locations of the intracellular domain 1 (ICD1) helices are also shown (dark gray). The Q-loop, which is indicated as a thick black loop, interacts with ICD1 helices and with the catalytic site. This figure was created using Molscript (*60*).

of basal activities seen in previous studies. Taken together, different studies can now be easily reconciled when the assay conditions, energy charge (and ATP concentrations), lipid membrane types employed, and potential polymorphisms are considered. For instance, we found that our results were in good agreement with the results of Müller et al. (*23*) when the differences of the factors discussed above were considered together.

Glycine is an important residue for protein conformation due to its high flexibility. Replacement of glycine with valine changes the main chain flexibility from the highest to almost lowest degree possible (*38*, *39*). A glycine to valine mutation in the catalytic loop of p21 oncogene protein changes local structure and resulted in altered function of the enzyme (*40*). In the case of influenza virus fusion peptide, mutation of alanine to glycine or valine changes secondary structure and function (*41*). Brandet-Rauf et al. (*42*) did computer simulations of local structure around P-glycoprotein residue 185 and found that the wild type had a unique left-handed conformation although G185V was a normal conformer. They concluded that a conformational change around this residue modifies drug binding. It is noteworthy that glycine is a potential helix disrupter and its replacement with valine may change local secondary structure around residue 185.

Although a crystal structure of human P-glycoprotein is not available, the analogous location of residue 185 in the structure of a bacterial homologue has special interest. We performed atomic detail structural homology modeling of human P-glycoprotein in a closed conformation. We employed the crystal structure of *Vibrio cholera* MsbA (*43*) together with the crystal structure of *E. coli* HisP (*44*) (Figure 7; see figure legend for modeling details). It was found that residue G185 is located in a kinked region at which transmembrane helix 3 (TM3) and intracellular domain 1 (ICD1) helices are connected. As the lipid A half-transporter MsbA is highly homologous with each half of P-glycoprotein (~27% identity), there are sound theoretical reasons to expect that the two proteins share considerable structural similarity (*45*). Furthermore, while this paper was under review, two different detailed structural homology models of human P-glycoprotein appeared. The first from Seigneuret and Garnier-Suillerot (*46*) was based on the crystal structure of *E. coli* MsbA in an open conformation (*47*). Their structure is different from Figure 7 in the orientation of nucleotide binding folds relative to the transmembrane domains. However, the closed conformation (as in Figure 7) is believed to be the active conformation (*43*) where the catalytic sites face each other, as is consistent with the available biochemical data. The second model from Stenham et al. (*48*) was based on the crystal structures of *E. coli* MsbA (*47*) and of *E. coli* HisP (*44*) constrained by disulfide cross-linking data. This latter model was very similar to the one in Figure 7. Overall, all three structural homology models agree that residue G185 is located in a kinked region where TM3 and ICD1 helices are connected.

The ICD1 helices interact with the Q-loop of the N-terminal catalytic site [Figure 7 (*47*, *49*)]. In another ATP binding cassette protein, Rad50 (*50*), a conserved glutamine residue in the Q-loop binds to the Mg^{2+} coordinated to ATP through oxygen atoms from β- and γ-phosphates of ATP. This close proximity to ATP indicates a central role for the Q-loop in ATP hydrolysis. Thus, the conformation of the

Q-loop would be sensitive to the events at the catalytic site. The Q-loop plays an essential role in transmitting information from/to the transmembrane helices through interactions with ICD1 helices (*49*, *51*, *52*). The results of Urbatsch et al. (*53*) employing mouse MDR3 P-glycoprotein support this hypothesis. They concluded that glutamines of the Q-loops are involved in interdomain communication between the nucleotide sites and drug binding sites. This is achieved by the Q-loops "transmitting conformational signals out of the catalytic site as the ATP hydrolysis transition state forms and collapses, to the coupling mechanism that ultimately generates transport-related conformational changes at the drug binding sites". This notion is consistent with our results and is also supported by mutational studies of the bacterial maltose transporter (*54*). In the human P-glycoprotein, mutations in these ICD1 helices yielded functionally deficient enzymes, further demonstrating a crucial role of this region for coupling (*55*).

When kinetic, transport, and thermodynamic parameters of G185C/Cys(−) Pgp are compared with its parental Cys(−) enzyme (Tables 1 and 2, Figures 2−4), G185C Pgp follows a similar tendency as G185V Pgp compared to wild-type Pgp. Such results suggest the importance of the side chain size at position 185. Our EPR data confirm this by indicating a tight packing state around residue 185. Together, these results indicate that residue 185 is a pivotal residue in conformational transmission between the transmembrane domain and the catalytic domain. Introduction of a bulky side chain to this position may affect the local conformation or flexibility, resulting in altered coupling mechanisms.

ACKNOWLEDGMENT

We thank Dr. Michael M. Gottesman for the kind gift of pSK1.MDR and Dr. David M. Clarke for sending us a cysteine-less MDR1 cDNA. We further thank Maria E. DiLorenzo and Dannon M. Smith for technical assistance. We are grateful to Dr. Eduardo Perozo for helpful discussions and for the use of his EPR spectrometer.

REFERENCES

1. Gottesman, M. M., and Pastan, I. (1993) Biochemistry of multidrug resistance mediated by the multidrug transporter, *Annu. Rev. Biochem. 62*, 385−427.
2. Hyde, S. C., Emsley, P., Hartshorn, M. J., Mimmack, M. M., Gileadi, U., Pearce, S. R., Gallagher, M. P., Gill, D. R., Hubbard, R. E., and Higgins, C. F. (1990) Structural model of ATP-binding proteins associated with cystic fibrosis, multidrug resistance and bacterial transport, *Nature 346*, 362−365.
3. Holland, I. B., and Blight, M. A. (1999) ABC-ATPases, adaptable energy generators fuelling transmembrane movement of a variety of molecules in organisms from bacteria to humans, *J. Mol. Biol. 293*, 381−399.
4. Senior, A. E., Al-Shawi, M. K., and Urbatsch, I. L. (1995) The catalytic cycle of P-glycoprotein, *FEBS Lett. 377*, 285−289.
5. Al-Shawi, M. K., Polar, M. K., Omote, H., and Figler, R. A. (2003) Transition state analysis of the coupling of drug transport to ATP hydrolysis by P-glycoprotein, *J. Biol. Chem. 278*, 52629−52640.
6. Choi, K. H., Chen, C. J., Kriegler, M., and Roninson, I. B. (1988) An altered pattern of cross-resistance in multidrug-resistant human cells results from spontaneous mutations in the mdr1 (P-glycoprotein) gene, *Cell 53*, 519−529.
7. Safa, A. R., Stern, R. K., Choi, K., Agresti, M., Tamai, I., Mehta, N. D., and Roninson, I. B. (1990) Molecular basis of preferential resistance to colchicine in multidrug-resistant human cells conferred by Gly-185 to Val-185 substitution in P-glycoprotein, *Proc. Natl. Acad. Sci. U.S.A. 87*, 7225−7229.
8. Stein, W. D., Cardarelli, C., Pastan, I., and Gottesman, M. M. (1994) Kinetic evidence suggesting that the multidrug transporter differentially handles influx and efflux of its substrates, *Mol. Pharmacol. 45*, 763−772.
9. Kane, S. E., Reinhard, D. H., Fordis, C. M., Pastan, I., and Gottesman, M. M. (1989) A new vector using the human multidrug resistance gene as a selectable marker enables overexpression of foreign genes in eukaryotic cells, *Gene 84*, 439−446.
10. Figler, R. A., Omote, H., Nakamoto, R. K., and Al-Shawi, M. K. (2000) Use of chemical chaperones in the yeast *Saccharomyces cerevisiae* to enhance heterologous membrane protein expression: high-yield expression and purification of human P-glycoprotein, *Arch. Biochem. Biophys. 376*, 34−46.
11. Loo, T. W., and Clarke, D. M. (1995) Membrane topology of a cysteine-less mutant of human P-glycoprotein, *J. Biol. Chem. 270*, 843−848.
12. Kim, R. B., Leake, B. F., Choo, E. F., Dresser, G. K., Kubba, S. V., Schwarz, U. I., Taylor, A., Xie, H. G., McKinsey, J., Zhou, S., Lan, L. B., Schuetz, J. D., Schuetz, E. G., and Wilkinson, G. R. (2001) Identification of functionally variant MDR1 alleles among European Americans and African Americans, *Clin. Pharmacol. Ther. 70*, 189−199.
13. Jones, E. W. (1991) Tackling the protease problem in *Saccharomyces cerevisiae*, *Methods Enzymol. 194*, 428−453.
14. Perlin, D. S., Harris, S. L., Seto-Young, D., and Harber, J. E. (1989) Defective H^+-ATPase of hygromycin B-resistant *pma1* mutants from *Saccharomyces cerevisiae*, *J. Biol. Chem. 264*, 21857−21864.
15. Urbatsch, I. L., Al-Shawi, M. K., and Senior, A. E. (1994) Charaterization of the ATPase activity of purified Chinese hamster P-glycoprotein, *Biochemistry 33*, 7069−7076.
16. Van Veldhoven, P. P., and Mannaerts, G. P. (1987) Inorganic and organic phosphate measurements in the nanomolar range, *Anal. Biochem. 161*, 45−48.
17. Al-Shawi, M. K., Ketchum, C. J., and Nakamoto, R. K. (1997) The *Escherichia coli* F_OF_1 gammaM23K uncoupling mutant has a higher $K_{0.5}$ for Pi. Transition state analysis of this mutant and others reveals that synthesis and hydrolysis utilize the same kinetic pathway, *Biochemistry 36*, 12961−12969.
18. Omote, H., and Al-Shawi, M. K. (2002) A novel electron paramagnetic resonance approach to determine the mechanism of drug transport by P-glycoprotein, *J. Biol. Chem. 277*, 45688−45694.
19. Al-Shawi, M. K., and Senior, A. E. (1988) Complete kinetic and thermodynamic characterization of the unisite catalytic pathway of *Escherichia coli* F_1-ATPase: Comparison with mitochondrial F_1-ATPase and application to the study of mutant enzymes, *J. Biol. Chem. 263*, 19640−19648.
20. Rao, U. S., and Nuti, S. L. (2003) Identification of two different states of P-glycoprotein in its catalytic cycle. Role of the linker region in the transition between these two states, *J. Biol. Chem. 278*, 46576−46582.
21. Ramachandra, M., Ambudkar, S. V., Gottesman, M. M., Pastan, I., and Hrycyna, C. A. (1996) Functional characterization of a glycine 185-to-valine substitution in human P-glycoprotein by using a vaccinia-based transient expression system, *Mol. Biol. Cell 7*, 1485−1498.
22. Rao, U. S. (1995) Mutation of glycine 185 to valine alters the ATPase function of human P-glycoprotein expressed in Sf9 cells, *J. Biol. Chem. 270*, 6686−6690.
23. Müller, M., Bakos, E., Welker, E., Varadi, A., Germann, U. A., Gottesman, M. M., Morse, B. S., Roninson, I. B., and Sarkadi, B. (1996) Altered drug-stimulated ATPase activity in mutants of the human multidrug resistance protein, *J. Biol. Chem. 271*, 1877−1883.
24. Liu, R., and Sharom, F. J. (1996) Site-directed fluorescence labeling of P-glycoprotein on cysteine residues in the nucleotide binding domains, *Biochemistry 35*, 11865−11873.
25. Krupka, R. M. (1999) Uncoupled active transport mechanisms accounting for low selectivity in multidrug carriers: P-glycoprotein and SMR antiporters, *J. Membr. Biol. 172*, 129−143.
26. Exner, O. (1973) The enthalpy−entropy relationship, *Prog. Phys. Org. Chem. 10*, 411−482.
27. Sharom, F. J., Yu, X., and Doige, C. A. (1993) Functional reconstitution of drug transport and ATPase activity in proteoliposomes containing partially purified P-glycoprotein, *J. Biol. Chem. 268*, 24197−24202.

28. Loo, T. W., and Clarke, D. M. (2002) Location of the rhodamine-binding site in the human multidrug resistance P-glycoprotein, *J. Biol. Chem. 277*, 44332−44338.
29. Blott, E. J., Higgins, C. F., and Linton, K. J. (1999) Cysteine-scanning mutagenesis provides no evidence for the extracellular accessibility of the nucleotide-binding domains of the multidrug resistance transporter P-glycoprotein, *EMBO J. 18*, 6800−6808.
30. Mchaourab, H. S., Lietzow, M. A., Hideg, K., and Hubbell, W. L. (1996) Motion of spin-labeled side chains in T4 lysozyme. Correlation with protein structure and dynamics, *Biochemistry 35*, 7692−7704.
31. Burbaum, J. J., Raines, R. T., Albery, W. J., and Knowles, J. R. (1989) Evolutionary optimization of the catalytic effectiveness of an enzyme, *Biochemistry 28*, 9293−9305.
32. Kioka, N., Tsubota, J., Kakehi, Y., Komano, T., Gottesman, M. M., Pastan, I., and Ueda, K. (1989) P-glycoprotein gene (MDR1) cDNA from human adrenal: normal P-glycoprotein carries Gly185 with an altered pattern of multidrug resistance, *Biochem. Biophys. Res. Commun. 162*, 224−231.
33. Ruth, A., Stein, W. D., Rose, E., and Roninson, I. B. (2001) Coordinate changes in drug resistance and drug-induced conformational transitions in altered-function mutants of the multidrug transporter P-glycoprotein, *Biochemistry 40*, 4332−4339.
34. Al-Shawi, M. K., Ketchum, C. J., and Nakamoto, R. K. (1997) Energy coupling, turnover, and stability of the F_0F_1 ATP synthase are dependent on the energy of interaction between gamma and beta subunits, *J. Biol. Chem. 272*, 2300−2306.
35. Nakamoto, R. K., Ketchum, C. J., and Al-Shawi, M. K. (1999) Rotational coupling in the F_0F_1 ATP Synthase, *Annu. Rev. Biophys. Biomol. Struct. 28*, 205−234.
36. King, S. C., and Wilson, T. H. (1990) Towards an understanding of the structural basis of 'forbidden' transport pathways in the *Escherichia coli* lactose carrier: mutations probing the energy barriers to uncoupled transport, *Mol. Microbiol. 4*, 1433−1438.
37. Botts, J., and Morales, M. (1953) Analytical description of the effects of modifiers and of enzyme multivalency upon the steady-state catalyzed reaction rate, *Trans. Faraday Soc. 49*, 696−707.
38. Ramachandran, G. N., and Sasisekharan, V. (1968) Conformation of polypeptides and proteins, *Adv. Protein Chem. 23*, 283−438.
39. Hovmoller, S., Zhou, T., and Ohlson, T. (2002) Conformations of amino acids in proteins, *Acta Crystallogr., Sect. D: Biol. Crystallogr. 58*, 768−776.
40. Tong, L. A., de Vos, A. M., Milburn, M. V., Jancarik, J., Noguchi, S., Nishimura, S., Miura, K., Ohtsuka, E., and Kim, S. H. (1989) Structural differences between a ras oncogene protein and the normal protein, *Nature 337*, 90−93.
41. Han, X., Steinhauer, D. A., Wharton, S. A., and Tamm, L. K. (1999) Interaction of mutant influenza virus hemagglutinin fusion peptides with lipid bilayers: probing the role of hydrophobic residue size in the central region of the fusion peptide, *Biochemistry 38*, 15052−15059.
42. Brandt-Rauf, P. W., Lee, G., Carty, R. P., Pincus, M. R., and Chen, J. M. (1989) Conformational effects of amino acid substitutions in the P-glycoprotein of the mdr 1 gene, *J. Protein Chem. 8*, 563−573.
43. Chang, G. (2003) Structure of MsbA from Vibrio cholera: a multidrug resistance ABC transporter homologue in a closed conformation, *J. Mol. Biol. 330*, 419−430.
44. Hung, L. W., Wang, I. X., Nikaido, K., Liu, P. Q., Ames, G. F.-L., and Kim, S. H. (1998) Crystal structure of the ATP-binding subunit of an ABC transporter, *Nature 396*, 703−707.
45. Yang, A. S., and Honig, B. (2000) An integrated approach to the analysis and modeling of protein sequences and structures. II. On the relationship between sequence and structural similarity for proteins that are not obviously related in sequence, *J. Mol. Biol. 301*, 679−689.
46. Seigneuret, M., and Garnier-Suillerot, A. (2003) A structural model for the open conformation of the mdr1 P-glycoprotein based on the MsbA crystal structure, *J. Biol. Chem. 278*, 30115−30124.
47. Chang, G., and Roth, C. B. (2001) Structure of MsbA from *E. coli*: A Homolog of the Multidrug Resistance ATP Binding Cassette (ABC) Transporters, *Science 293*, 1793−1800.
48. Stenham, D. R., Campbell, J. D., Sansom, M. S., Higgins, C. F., Kerr, I. D., and Linton, K. J. (2003) An atomic detail model for the human ATP binding cassette transporter P-glycoprotein derived from disulfide cross-linking and homology modeling, *FASEB J. 17*, 2287−2289.
49. Locher, K. P., Lee, A. T., and Rees, D. C. (2002) The *E. coli* BtuCD structure: a framework for ABC transporter architecture and mechanism, *Science 296*, 1091−1098.
50. Hopfner, K. P., Karcher, A., Shin, D. S., Craig, L., Arthur, L. M., Carney, J. P., and Tainer, J. A. (2000) Structural biology of Rad50 ATPase: ATP-driven conformational control in DNA double-strand break repair and the ABC-ATPase superfamily, *Cell 101*, 789−800.
51. Jones, P. M., and George, A. M. (2002) Mechanism of ABC transporters: a molecular dynamics simulation of a well characterized nucleotide-binding subunit, *Proc. Natl. Acad. Sci. U.S.A. 99*, 12639−12644.
52. Schmitt, L., and Tampe, R. (2002) Structure and mechanism of ABC transporters, *Curr. Opin. Struct. Biol. 12*, 754−760.
53. Urbatsch, I. L., Gimi, K., Wilke-Mounts, S., and Senior, A. E. (2000) Investigation of the role of glutamine-471 and glutamine-1114 in the two catalytic sites of P-glycoprotein, *Biochemistry 39*, 11921−11927.
54. Mourez, M., Hofnung, M., and Dassa, E. (1997) Subunit interactions in ABC transporters: a conserved sequence in hydrophobic membrane proteins of periplasmic permeases defines an important site of interaction with the ATPase subunits, *EMBO J. 16*, 3066−3077.
55. Currier, S. J., Kane, S. E., Willingham, M. C., Cardarelli, C. O., Pastan, I., and Gottesman, M. M. (1992) Identification of residues in the first cytoplasmic loop of P-glycoprotein involved in the function of chimeric human MDR1-MDR2 transporters, *J. Biol. Chem. 267*, 25153−25159.
56. Fiser, A., Do, R. K. G., and Sali, A. (2000) Modeling of loops in protein structures, *Protein Sci. 9*, 1753−1773.
57. Higgins, D. G., and Sharp, P. M. (1988) CLUSTAL: a package for performing multiple sequence alignment on a microcomputer, *Gene 73*, 237−244.
58. Rost, B., and Sander, C. (1993) Secondary structure prediction of all-helical proteins in two states, *Protein Eng. 6*, 831−836.
59. Rost, B. (1996) PHD: predicting one-dimensional protein structure by profile-based neural networks, *Methods Enzymol. 266*, 525−539.
60. Kraulis, P. J. (1991) A program to produce both detailed and schematic plots of protein structures, *J. Appl. Crystallogr. 24*, 946−950.

BI035365L